Supplementary data

Identification of small molecules that suppress microRNA pathway and reverse tumorigenesis

Koichi Watashi, Man Lung Yeung, Matthew F. Starost, Ramachandra S. Hosmane, and Kuan-Teh Jeang

Supplementary Figures S1-8 and legends
Supplementary Table

Supplementary Fig. S1.

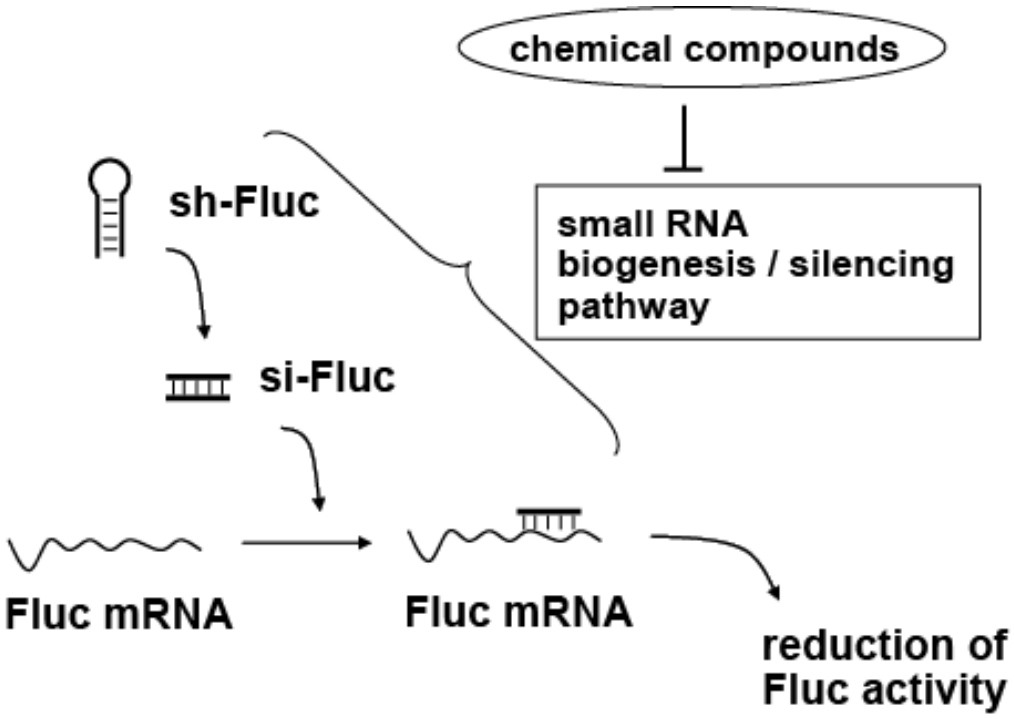

Supplementary Fig. S1. Schematic representation of the strategy for identifying compounds that suppress small RNA biosynthesis/silencing pathway.

Supplementary Fig. S2.

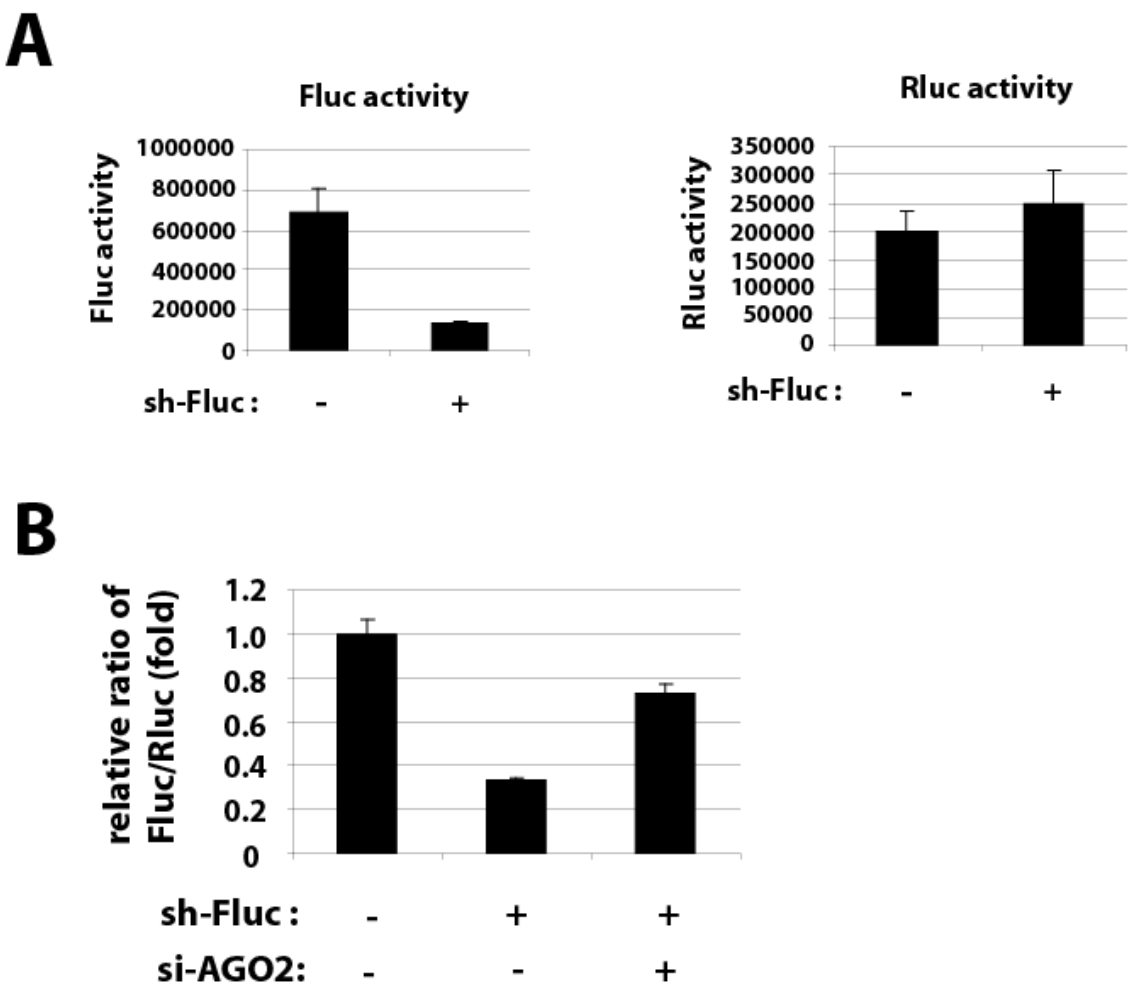

Supplementary Fig. S2. Specificity of sh-Fluc suppression of Fluc activity. (A) sh-Fluc (shRNA targeting firefly luciferase mRNA) suppressed the activity of Fluc (firefly luciferase) but not Rluc (renilla luciferase). 293T cells transfected with pGL3 (Fluc plasmid), pRL-TK (Rluc plasmid), and pRS-shLuc (sh-Fluc +) or pRS control vector (sh-Fluc -) were measured for Fluc (left) and Rluc activities (right). (B) Knockdown of endogenous AGO2 reversed shRNA-mediated gene silencing. 293T cells were transfected without (si-AGO2 -) or with (si-AGO2 +) siRNA targeting AGO2. After 24 hrs, the cells were transfected with pGL3 (Fluc), pRL-TK (Rluc), and pRS-shLuc (sh-Fluc +) or pRS control vector (sh-Fluc -). After a further 24 hrs, cells were harvested and detected for Fluc and Rluc activities. Relative ratios of Fluc/Rluc are shown.

Supplementary Fig. S3.

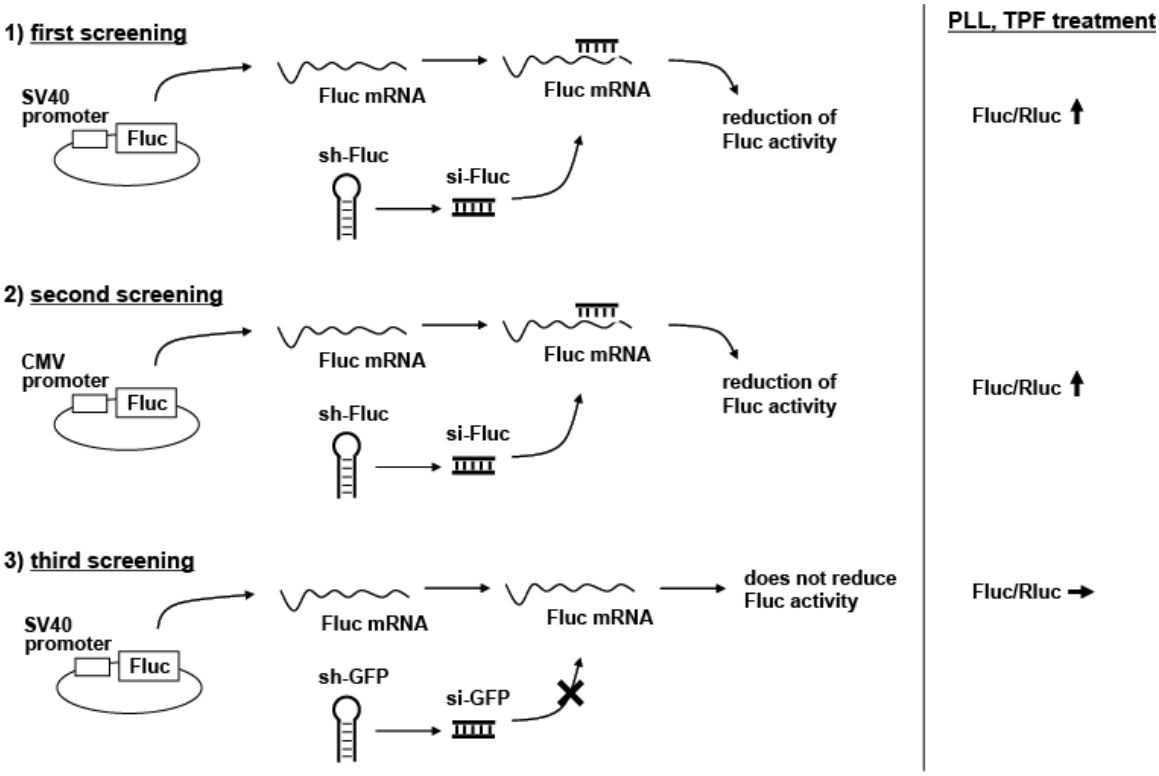

Supplementary Fig. S3. The various screening steps and their outcomes. 1) In the first screening, 293T cells were transfected with SV40 promoter-driven Fluc, Rluc, and sh-Fluc, and then treated with individual compounds from the library. 2) The second screening employed a Fluc cDNA driven from a CMV promoter instead of the SV40 promoter. This screening is designed to identify compounds that affect Fluc activity irrespective of the promoter that drives Fluc expression. 3) In the third screening, sh-GFP, which recognizes GFP mRNA, but not Fluc mRNA was used as a negative-control shRNA to rule out non-specific shRNA effects that might affect Fluc activity. In this figure, Rluc is not shown to simplify the schematic presentation. Treatment of transfected cells with PLL and TPF increased the Fluc/Rluc ratio in the first and second screening procedures, but not in the third screening (right).

Supplementary Fig. S4.

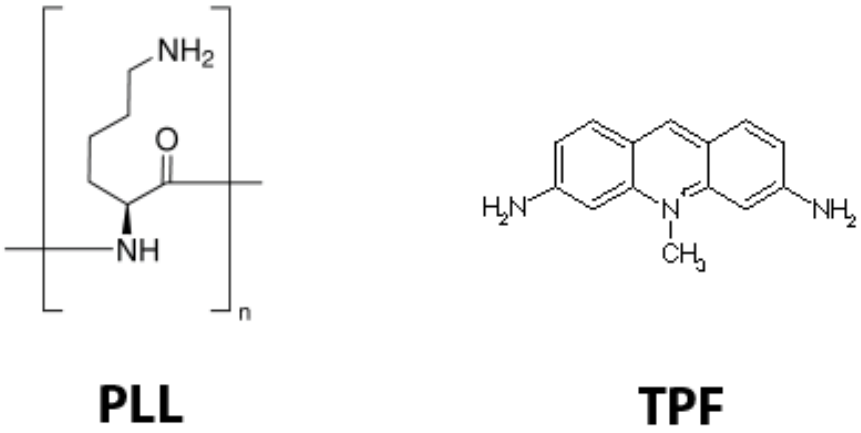

Supplementary Fig. S4. The structures of PLL (poly-L-lysine) and TPF (trypaflavine), two moieties identified from our screening of 530 compounds

Supplementary Fig. S5.

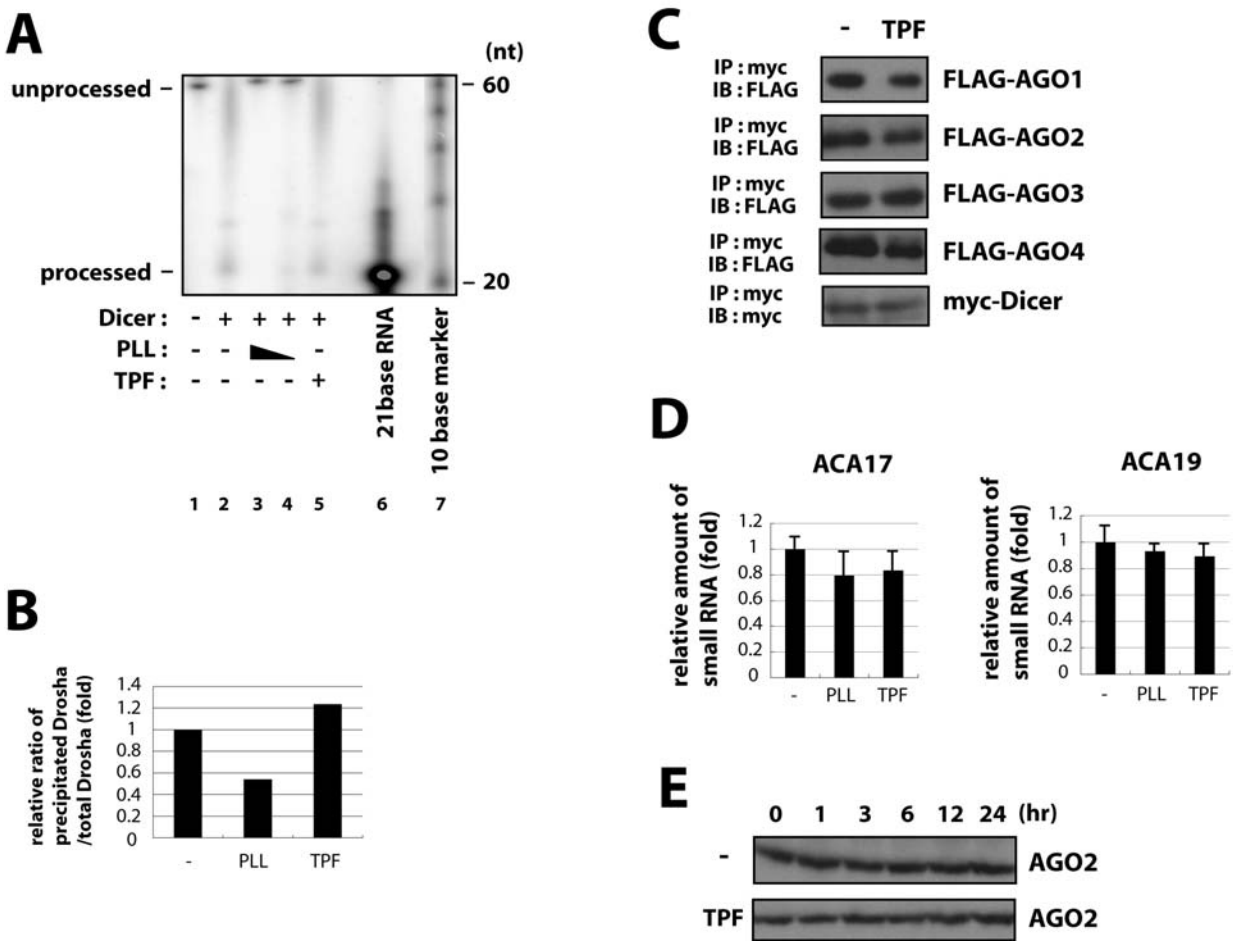

Supplementary Fig. S5. Assays for PLL and TPF activities in cell lysates and cultured cells. (A) *In vitro* Dicer assay. Pre-let-7a RNA was labeled with ^{32}P and incubated with (lanes 2-5) or without (lane 1) Dicer in the presence of PLL (8 and 4 μM; lanes 3 and 4) or TPF (100 μM; lane 5). (B) In vitro RNA precipitation assays employing biotinylated pre-let-7a RNA in 293T cells over expressing myc-Drosha were performed as in Fig. 2D. The amount of Drosha protein associated with biotinylated RNA was quantified from untreated(-), PLL, or TPF- treated cells. ***(***C) 293T cells overexpressing myc-Dicer were individually transfected with FLAG-AGO1, 2, 3, or 4, and the cells were treated with TPF or untreated (-). Each of the individually transfected cells was immunoprecipitated with anti-myc antibody followed by immunoblot detection with anti-FLAG or anti-myc antibody. The bottom myc-Dicer immunoblot panel is a representative result reflective of the anti-myc IP followed by anti-myc IB seen with each of the FLAG-AGO1, 2, 3, 4 transfected cells. (D) snoRNAs, ACA17 and ACA19 were quantified by real time RT-PCR analysis in 293T cells treated with PLL, TPF, or untreated. (E) The stability of endogenous AGO2 in TPF-treated or untreated (-) 293T cells was detected by immunoblotting with anti-AGO2 after cycloheximide treatment for 1, 3, 6, 12, and 24 hrs.

Supplementary Fig. S6.

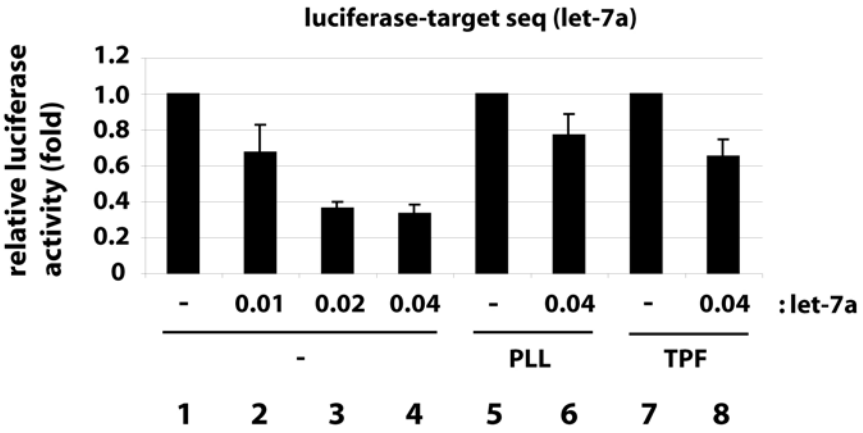

Supplementary Fig. S6. PLL and TPF reversed the silencing activity of let-7a. A plasmid encoding firefly luciferase (Fluc) mRNA carrying three repeats of the target sequence for let-7a positioned in its downstream untranslated sequences was transfected into HeLa cells together with an expression plasmid for renilla luciferase (Rluc) and the indicated amounts (μg) of let-7a expression plasmid. After 4 hours, cells were treated with PLL or TPF. After another 48 hours, cells were lysed and luciferase activities were quantified. The relative activities of Fluc/Rluc are shown after setting the value in lane 1 as 1.

Supplementary Fig. S7.

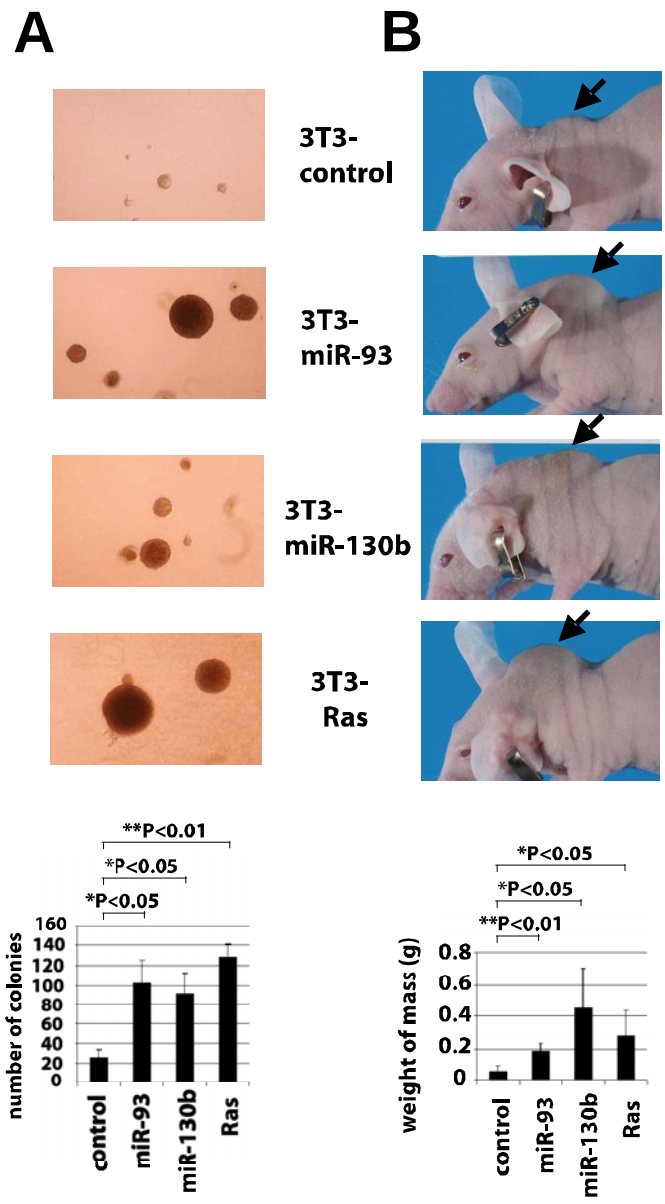

Supplementary Fig. S7. A cell-mouse model for miR-93 and -130b-dependant tumorigenesis. (A) NIH3T3 cells stably over expressing miR-93 (3T3-miR-93), -130b (3T3-miR-130b), or Ras (3T3-Ras), or control (3T3-control) cells with an empty vector (3T3-control) were assayed for focus formation in soft agar. Microscopy (upper) and graphic tabulation of colonies (bottom) are shown. 3T3-miR-93 and 3T3-miR-130b as well as 3T3-Ras produced significantly higher numbers of colonies than control. (B) 3T3-control, 3T3-miR-93, 3T3-miR-130b, and 3T3-Ras cells were implanted into nude mice subcutaneously in the back of the neck and observed for tumor formation. Pictures of the mice (upper) and the average weights of tumor masses dissected from the animals after necropsy (bottom) are shown.

Supplementary Fig. S8.

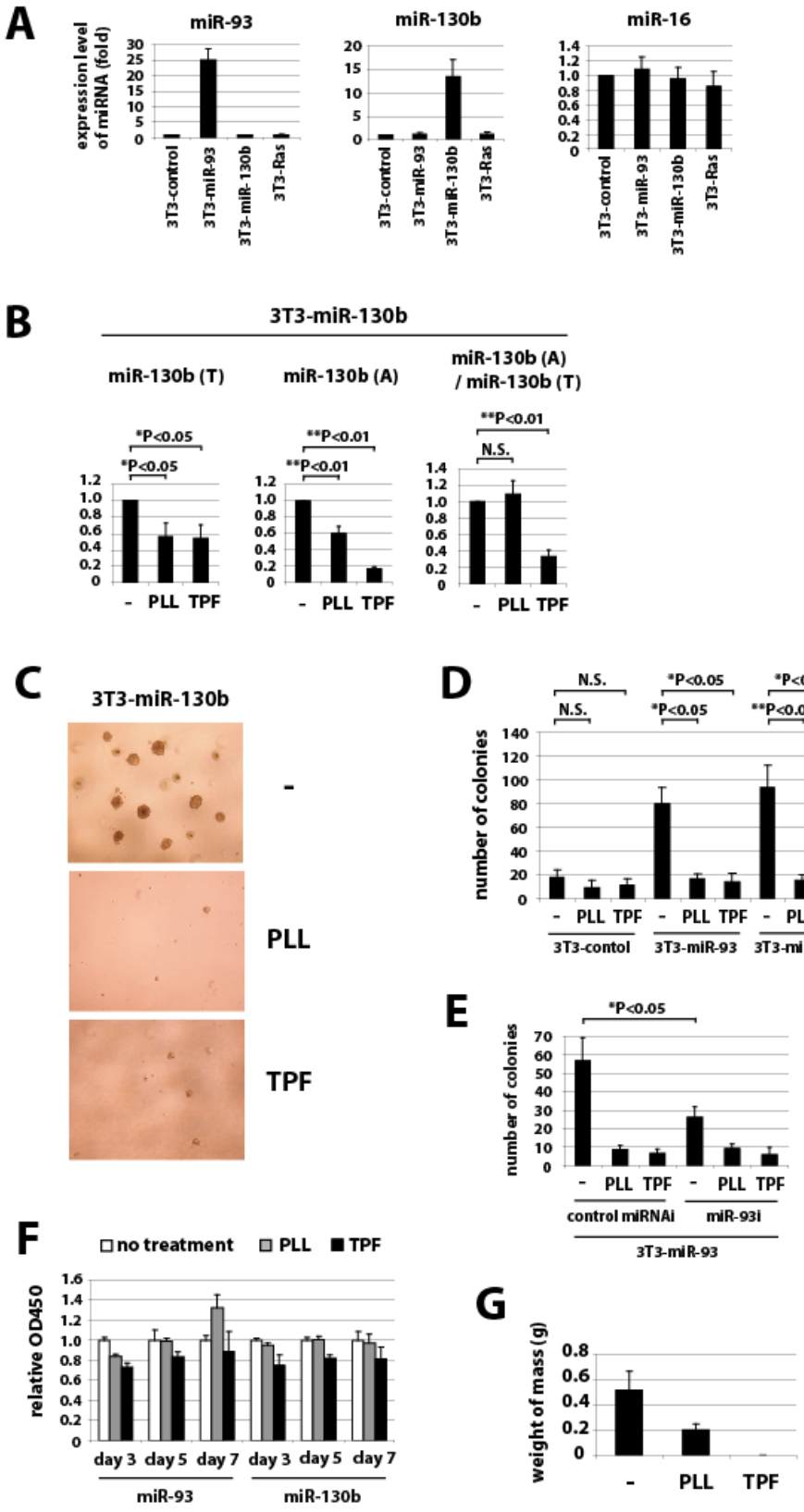

Supplementary Fig. S8. PLL and TPF treatment reduced the tumorigenic activity of miR-93 and -130b. (A) miR-93, miR-130b, and miR-16 (as a control) were quantified in 3T3-control, 3T3-miR-93, 3T3-miR-130b, and 3T3-Ras cells by real time RT-PCR analyses. (B) 3T3-miR-130b cells transfected with FLAG-AGO2 were treated with PLL or TPF, or were untreated (-) for 3 days, and then the cells were recovered for small RNAs as described in Fig. 6A. MiR-130b in the miRNA(T) and the miRNA(A) fractions were quantified, and the ratios of miRNA(A)/miRNA(T) are shown. (C) 3T3-miR-130b cells treated with 2 μM PLL, 1 μM TPF, or untreated (-), were observed in soft agar growth assays as described in Fig. 6B. Representative images are shown. (D) Colony formation assays were performed with 3T3-control, 3T3-miR-93, 3T3-miR-130b, and 3T3-Ras cells treated with PLL, TPF, or untreated, as described in Fig. 6B. Numbers of colonies were counted and shown. (E) 3T3-miR-93 cells transfected with antagonizing oligonucleotide for miR-93 (miR-93i) or a randomized oligonucleotide (control miRNAi) were subjected to colony formation assay as described in Fig. 6B. Numbers of colonies were counted and shown. (F) MTT assays of 3T3-miR-93 and 3T3-miR-130b cells treated with 2 μM PLL, 1 μM TPF, or untreated at days 3, 5, and 7 post treatment. (G) The average weights of tumor masses for the results in Fig. 6C are shown.

Supplementary Table. Names of chemical compounds screened in this study.

A23187
17-AAG
AB-112
AB-120
AB-122
AB-124
AB-13
AB-150
AB-160-OMe
AB-161
AB-162
AB-166
AB-166B
AB-171
AB-173
AB-174
AB-175
AB-176
AB-18
AB-180
AB-185
AB-186
AB-2
AB-200
AB-203
AB-213
AB-214
AB-221
AB-222
AB-260
AB-3
AB-31
AB-32
AB-43
AB-49
AB-5
AB-53
AB-55
AB-57
AB-61
AB-63
AB-64
AB-66
AB-67
AB-68
AB-82
AB-85
AB-87A
AB-9
AB-RSH-1
AB-RSH-11
AB-RSH-2
AB-RSH-4
AB-RSH-5
AB-RSH-6
AB-RSH-7
AB-RSH-9
ABR-1
ABR-6
ABR-8
ABRSH-5
ABRSH-6
ABRSH-10H
Aclarubicin
acetic acid
Actinomycin D
Actinonin
ADP
AG1024
AG1296
AG1478
AG490
AG825
AG957
ALLN
a-Amanitin
Amastatin
AMD3100
Amiloride
1-aminoanthracene
2-aminoanthracene
Aminoglutethimide
Aminoguanidine
AMT
Anacardic acid
Antimycin A1
Aphidicolin
AR-1
AR-104
AR-122
AR-19
AR-2
AR-20
AR-3
AR-4
AR-5
AR-6
AR-61
AR-RSH-1
arachidonic acid
arsenate
arsenite
3-ATA
ATRA
Azacytidine
AZT
Baicalein
Bafilomycin A1
BAPTA-AM
BBL-1
BBL-116
BBL-128
BBL-132
BBL-135
BBL-13
BBL-159
BBL-161
BBL-19
BBL-228
BBL-32
BBL-37
BBL-37-1R
BBL-38-18R
BBL-43
BBL-44
BBL-5
BBL-59
BBL-65
BBL-66
BBL-67
BBL-78
BBL-RSH-1
BBL-RSH-2
Benzamide
Benzylguanine
Bestatin
bFGF
Bisindolymaleimide I
Bisphenol A diglycidyl ether
BKA
blasticidin
Bleomycin
BMP4
t-Butylhydroquinone
C75
CA-074
calpeptin
Camptothecin
Cantharidin
CAT
CB-10
CB-129
CB-45
2CB-202
3-CB-85
6-CB-59
6-CB-79
7-CB-178
Cerulenin
Cisplatin
Clofibrate
CPA
9cRA
Cucurbitacin I
Cycloheximide
Cyclosporin A
Cytochalasin D
Damnacanthal
Daunorubicin
Decylubiquinone
Deoxynojirimycin
Dephostatin
Deprenyl
Dequalinium
Dexamethasone
DFMO
Diazoxide
2',5'-dideoxyadenosine
DIDS
Diltiazem
DMSO
Doxorubicin
E-64d
EGF
ethanol
Etoposide
ETYA
Finasteride
FK-506
Flutamide
fluvastatin
Formestane
FTI-276
5-FU
Fumagillin
Fumitremorgin C
Fumonisin B1
geneticin
Genistein
gentamicin
GGTI-286
Glibenclamide
GM 6001
Go6976
H-7
H-89, HCl
HA 14-1
HMC-RSH-12
HMC-RSH-16
HMC-RSH-2
HMC-RSH-26
HMC-RSH-27

Supplementary Table (continued).

HMC-RSH-29	L-NMMA	Phenelzine	SP-131
HMC-RSH-3	Lonidamine	N-phenylanthranilic acid	SP-133
HMC-RSH-30	Lovastatin	Pifithrin-a (cyclic)	SP-136
HMC-RSH-31	LY294002	PMA	SP-137
HMC-RSH-32	LY 83583	polyarginine	SP-138
HMC-RSH-33	Manumycin A	polylysine	SP-139
HMC-RSH-36	Methotrexate	PRIMA-1	SP-141
HMC-RSH-37	methylene blue	proflavin	SP-144
HMC-RSH-41	MG-132	puromycin	SP-146
HMC-RSH-42	Mifepristone	Purvalanol A	SP-159
HMC-RSH-44	Mitomycin C	quinacrine	SP-196
HMC-RSH-45	MK 886	R59022	SP-197
HMC-RSH-5	ML-7	Radicicol	SP-199*
HMC-RSH-51	Monastrol	Rapamycin	SP-212
HMC-RSH-53	Monensin	RHC80267	SP-217
HMC-RSH-57	MPA	riboflavin	SP-225
HMC-RSH-58	MST-312	RK-05	SP-227
HMC-RSH-61	N-Acetyl-L-cysteine	RK-06	SP-3*
HMC-RSH-62	Nalidixic acid	RK-07	SP-35
HMC-RSH-66	NB-DNJ	RK-33	SP-36*
HMC-RSH-67	NEM	RK-40	SP-39*
HMC-RSH-71	Nifedipine	RK-48	SP-43
HMC-RSH-72	Nigericin	RK-52	SP-45
HMC-RSH-75	Nocodazole	RKP-04	SP-47
HMC-RSH-76	Nordihydroguaiaretic acid	RKP-08	SP-48
HMC-RSH-77	NS-398	RKP-09	SP-51
HMC-RSH-78	NS-1	RKP-09a	SP-6
HMC-RSH-79	NS-1'	Ro-20-1724	SP600125
HMC-RSH-8	NS-2	Ro 5-4864	Staurosporine
HMC-RSH-9	NS-3	Rotenone	SU1498
4-OH tamoxifen	NS-3'	Rp-8-CPT-cGMPS	Sulindac
Hydroxyurea	NS-4	RSH-004	Swainsonine
hygromycin B	NS-6	RSH-005	Tamoxifen
IBMX	Nutlin-3	RSH-009	TBB
IFNa	NZ28	RSH-012	TFP
IFNb	NZ48	RSH-019	TGF-b2
IFNg	NZ49	RSH-020	Thapsigargin
IGF1	NZ50	RSH-027	Theophylline
IL-1b	NZ51	RSH-117	thymidine
IL-6	NZ-53	RSH-161A	TNFa
insulin	ODQ	RSH-6101	To-901317
Ionomycin	Oligomycin	salicylate	TOFA
IPTG	Olomoucine	Sanguinarine	TR-079
juglone	Ouabain	SB 203580	TR-175
kanamycin	Paclitaxel	SB 431542	TR-191
Kenpaullone	PAO	SC560	TR-196
KN93	PD169316	SP-102*	TR-197
KT 5823	PD 98059	SP-116	TR-251
Lactacystin	PDGF-AA	SP-119	TR-253
Leptomycin B	PDGF-BB	SP-120	TR-255
LFM-A13	Pepstatin A	SP-121	TR-264
Lidocaine	PGA1	SP-122	TR-267
lithium chloride	PHA	SP-128	TR-268

Supplementary Table (continued).

TR-269
TR-270
TR-272
TR-275
TR-280
TR-281
TR-291
TR-601
TR-609
TR-610
TR-90
TR-91
TR-94
TR-96
Trichostatin A
Troglitazone
trypafravine
Tunicamycin
U0126
UMR-101a
UMR-101b
UMR-103
UMR-104a
UMR-104b
UMR-118
UMR-120
UMR-121
UMR-126
UMR-127
UMR-164
UMR-20
UMR-22
UMR-38
UMR-63
Valeryl salicylate
Valinomycin
Verapamil
Vinblastine
VK-1
VK-100
VK-102
VK-103
VK-106
VK-120
VK-2
VK-24
VK-25
VK-26
VK-27
VK-3
VK-32
VK-4
VK-4-OPFP
VK-5
VK-5dimer
VK-5NH2
VK-50
VK-52
VK-53
VK-54
VK-6
VK-6A
VK-6B
VK-6C
VK-6X
VK-7
VK-7C
VK-75
VK-8
VK-RSH-1
VK-RSH-10
VK-RSH-12
VK-RSH-16
VK-RSH-18
VK-RSH-2
VK-RSH-20
VK-RSH-22
VK-RSH-3
VK-RSH-6
VK-RSH-7
1400W, HCl
Wortmannin
Xanthohumol
Zaprinast
ZP-110
ZP-121
ZP-122
ZP-147
Z-VAD-FMK